Three-Dimensional Vibrational Study of the Coupling between Methyl Torsion and the Molecular Frame in the So State of Acetaldehyde

ARTICLE *in* THE JOURNAL OF PHYSICAL CHEMISTRY B · APRIL 2002

Impact Factor: 3.3 · DOI: 10.1021/j100021a010

3 AUTHORS:

Alfonso Niño
University of Castilla-La Mancha
104 PUBLICATIONS **848** CITATIONS
SEE PROFILE

Camelia Muñoz-Caro
University of Castilla-La Mancha
100 PUBLICATIONS **832** CITATIONS
SEE PROFILE

David Moule
Brock University
159 PUBLICATIONS **1,739** CITATIONS
SEE PROFILE

A conformational study of the $S_1(n,\pi^*)$ excited state of formic acid

Leanne M. Beaty-Travis and David C. Moule
Department of Chemistry, Brock University, St. Catharines, Ontario, L2S 3A1, Canada

Edward C. Lim[a)]
Department of Chemistry and Center for Laser and Optical Spectroscopy, The University of Akron, Akron, Ohio 44325-3601

Richard H. Judge
Department of Chemistry, University of Wisconsin-Parkside, Kenosha, Wisconsin 53141-2000

(Received 10 April 2002; accepted 11 June 2002)

Recent high resolution data from the vibronic bands in the $S_1 \leftarrow S_0$ electronic transition in HCOOH were combined with UMP2 *ab initio* calculations to establish the torsion-wagging potential energy surface over $\theta = \pm 90°$ for the torsional coordinate and $\alpha = \pm 60°$ for the wagging angle for the S_1 electronic state. The separations between the *c*- and *a*/*b*-type band origins were used to establish a global maximum of 5275 cm^{-1} for the torsion-wagging potential function. The stability of the structural conformers in the S_1 state was obtained from the vibrational intervals in the OH torsional progression that were fitted to the levels calculated from a two dimensional torsion-wagging vibrational model. The fitted potential surface revealed a pair of stable conformers with minima at $\theta = +68.08$, $\alpha = +57.51$ and $\theta = -68.08$, $\alpha = -57.51$ deg. A second pair of conformers with minima at $\theta = -48.50$, $\alpha = +44.77$ or $\theta = +48.50$, $\alpha = -44.77$ deg was found to be 1207 cm^{-1} less stable and to be separated by a torsional saddle point of 1270 cm^{-1} from the more stable conformers. © *2002 American Institute of Physics.* [DOI: 10.1063/1.1497632]

I. INTRODUCTION

Formic acid, HCOOH, is the simplest of the organic acids and thus is a prototype in the series of carboxylic acid molecules. In the S_0 ground electronic state, the equilibrium structure is planar and the two hydrogens point away from each other and form the antirotamer (conformer). With the 180° rotation of the hydroxy hydrogen about the O–C single bond, a second planar structure is created, the syn-rotamer. Figure 1 shows the arrangement. The energetics of this OH group internal rotation in formic acid has played a prominent role in the early studies of rotational isomerism.[1] The structure and dynamics of the low frequency modes in the first singlet excited state of formic acid are less well known. This $S_1(n\pi^*)$ state is the consequence of an excitation of an electron from the *n* nonbonding orbital on the oxygen atom to the antibonding π^* orbital in the carbonyl group. It thus can be accessed by the technique of electronic spectroscopy through an $n \rightarrow \pi^*$ electron promotion. It was recognized very early on that the $S_1 \leftarrow S_0$ electronic spectrum of formic acid possessed a rich vibrational structure in the 268–257 nm near the UV region that became diffuse at higher energies and eventually merged into a continuum.[2] The first serious attempt to analyze this system was made by Ng and Bell,[3] who used long path lengths to record the weaker bands in absorption at the red end of the spectrum. Band congestion at room temperature prevented these workers from assigning the quantum numbers to the vibrational structure, though they were able to perform rotational band contour analyses and show that the bands were of *a*/*b*/*c* hybrid character.

The solution to the problem of the vibrational assignments and the location of the 0_0^0 origin band came from laser induced fluorescence (LIF) excitation spectroscopy. In 1990 we recorded[4] the spectrum under bulb conditions (room temperature) and found that much of the underlying interfering continuum and diffuse hot band structures were eliminated under excitation conditions. We were able to locate progressions in the spectrum that could be assigned to the activity of the hydroxy low frequency torsional mode, Q_9. These progressions were observed to attach to the 0_0^0 system origin, the first quantum of the O–C═O bend, Q_7, the C═O stretch, Q_3 and the acetyl hydrogen out-of-plane mode, Q_8. From the activity of the vibrational modes it was clear that the upper electronic state was nonplanar at the hydroxy and torsional ends of the molecule with the OH group rotating out from the O–C═O frame (plane) and the CH group undergoing a wagging pyramidalization. In a continuation of this series, we recorded the excitation spectrum under higher resolution and the cooling conditions of a rotating slit jet nozzle. From a line-by-line and band contour analyses we were able to fit the rotational structure of the stronger bands to an asymmetric top model and establish the separations between the *a*/*b*- and *c*-type band origins.[5] In a sequel to this work[6] we employed RHF/UHF *ab initio* calculations and showed that the hydrogen atoms assume a nonplanar equilibrium conformation in the upper electronic state and project from the opposite sides of the O–C═O plane.

Our purpose here is to extend the understanding of the conformational behavior of the S_0 and S_1 states from an

[a)]Holder of the Goodyear Chair in Chemistry at The University of Akron. Fax: 330-972-6407. Electronic mail: elim@uakron.edu

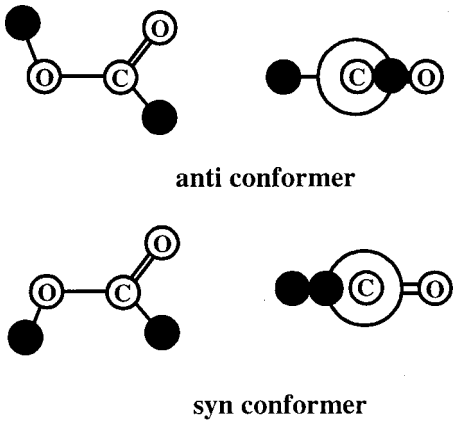

FIG. 1. The two stable conformers of HCOOH in the S_0 ground electronic state. Plan view (left) and Newman projections viewed along the C–O axis. Hydrogen atoms are denoted as black circles.

analysis of the torsional-wagging vibronic band structure. Such analyses would provide information about the location of the minima (equilibrium positions), the saddle points and the barrier heights (maxima) to torsion-wagging inversion.

II. THE VIBRATIONAL SPECTRUM

Figure 2 gives an overview of the LIF excitation spectrum recorded under slit jet conditions. The prominent band at 37 413.39 cm^{-1} (0.00 cm^{-1}, relative) is clearly the 0_0^0 electronic origin and forms the starting point for the dominant progression in the OH torsional mode, Q_9. The strength of first vibrational band at +250.83 cm^{-1} to higher energies, that forms the first member of the torsional progression, 9_0^1, is an indication of the significant structural differences between the two states. The second and third members of this series, 9_0^2 and 9_0^3 are observed at +377.20 and +513.6 cm^{-1}. What is notable in this progression is the remarkable anharmonicity in the first two intervals, 250.83 and 126.37 cm^{-1}. This same progression is observed to attach to a weak band at 404 cm^{-1} that has been attributed to a quantum addition of the O–C═O bending mode, Q_7.[4]

The identification of the C═O stretching mode, Q_3, should be straightforward. However, the fluorescence emission breaks off very early on in the spectrum and band progressions at higher energies cannot be identified. As there are a number of candidates in the spectrum for the assignment of the 3_0^1 transition, we turned to a correlation of the carbonyl

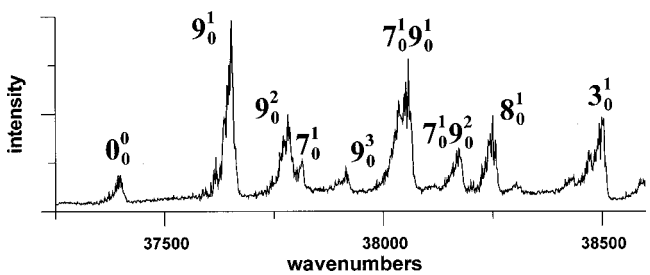

FIG. 2. The low-resolution excitation spectrum of HCOOH along with vibrational assignments. Q_8 and Q_9 represent the wagging and torsional coordinates, respectively.

TABLE I. Observed bands in the $S_1 \leftarrow S_0$ excitation spectrum of HCOOH (in cm^{-1}).

Assignment	Origin (+)[a]	Origin (−)[b]	Head[c]
0_0^0	37 413.39	37 413.39	37 431
9_0^1	37 664.22	37 664.22	37 682
9_0^2	37 790.61	37 790.90	37 810
7_0^1			37 835
9_0^3			37 945
$7_0^1 9_0^1$			38 094
$7_0^1 9_0^2$			38 218
8_0^1	38 279.69	38 280.20	38 297
3_0^1			38 546

[a]*c*-type transition Ref. 5.
[b]*a*/*b*-type transition Ref. 5.
[c]Low resolution, from Ref. 4.

stretching frequencies in the similar molecules, HFCO (Ref. 7) and HClCO.[8] In this pair of molecules, the excited to ground state S_1/S_0 fundamentals vary as 1112/1837 (cm^{-1}) for HFCO and 1154/1784 (cm^{-1}) for HClCO. As the S_0 ground state C═O fundamental in formic acid[1] has been measured to be 1770 cm^{-1}, an interpolation of the above data allowed us to assign the band observed at +1115 cm^{-1} to 3_0^1. The OH yield spectrum of Simons and co-workers[9] maps out the higher energy region of the spectrum and in particular the torsional bands attached to the third and fourth members of the C═O progression, 3_0^3 and 3_0^4. What is of interest is that the band patterns in the OH yield spectrum at higher energy replicate those attached to the 0_0^0 origin band, and thus gives credence to the present band assignments.

The remaining band in this region, at +866 cm^{-1}, can be assigned to the acetyl hydrogen mode, Q_8. The assignment of this band comes from a correlation to HFCO (Ref. 7) and HClCO (Ref. 8), where the wagging fundamental frequencies are observed at 746 and 779 cm^{-1}, respectively. The observed data are collected together in Table I.

III. ANALYSIS

The general procedure that is followed in this section is to employ a RHF/UHF *ab initio* methodology to establish a set of torsion-wagging energy levels for the two electronic states. Band positions are derived from the calculated levels and are then fitted to the observed positions by adjusting the coefficients that define the shape of the potential functions. This is a morphing procedure whereby the potential functions initially derived by *ab initio* methods are adjusted until the calculated levels are brought into agreement with the observed frequency data. As the torsion-internal rotation of the hydroxy hydrogen and the wagging-inversion of the acetyl group describe the large amplitude vibrations of the S_1 excited state, the model needs to be formulated in terms of these two motions. These internal coordinates, θ (torsion) and α (wagging) are defined in Fig. 3. Fully optimized *ab initio* calculations with the GAUSSIAN 95 program[10] were used to establish a grid of energy data points that define the potential functions. For the one-dimensional calculations, the grid points were taken at 30° intervals in *q* and 10° intervals in *a*. Extra points were added to the plots in the region of

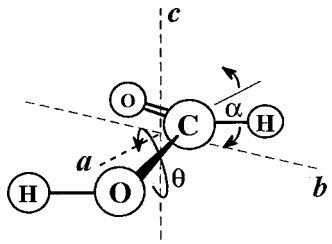

FIG. 3. The definition of the OH torsion (θ), the CH wagging coordinates (α), and the *a*, *b*, and *c* principal axes.

equilibrium positions for the two conformers. These data points were reduced to analytical form by fitting the energy calculated at each point to a function containing polynomic or Fourier terms. The expansion for the potential takes the form,

$$V=\sum_{k}^{N_v} V_k^0 \prod_{j}^{n} f_{kj}, \tag{1}$$

where V_k^0 are coefficients obtained from the fitting of the above equation to the calculated energy points while the f_{kj} represent the trigonometric (torsion) or polynomic (wagging) variables. N_v is the number of terms in the expansion while the product is taken over the internal coordinates ($n=1$ for pure torsion and 2 for torsion-wagging). The order of the terms and their composition were determined by the fitting procedure that mapped the surface established by an analytical expansion to the surface calculated from the UMP2/6-31G(d,p) procedure. This is the most difficult part of the morphing process and it does require a degree of judgment as to which terms to employ. This process is aided by the SPSS statistical package that automatically removes the additional terms that do not contribute to the fit. In general, an undulating potential surface requires more expansion terms than a smooth surface. The kinetic energy contributions were generated in a somewhat similar way from the fully optimized geometries at each of the θ and α points as the elements of the rovibrational G matrix.[11] B_{ijk}^0 are the coefficients obtained from the fit of Eq. (2) to the points on the grid. N_B is the number of terms in the expansion for the kinetic energy,

$$B_{ij}=\sum_{k}^{Nv} B_{ijk}^0 \prod_{l}^{n} f_{ijkl}. \tag{2}$$

The general Hamiltonian[12] was used for the treatment of the multidimensional vibrational problem,

$$\hat{H}=\sum_{i}^{n}\sum_{j}^{n}\left(-B_{ij}\frac{\partial^2}{\partial q_i \partial q_j}-\frac{\partial B_{ij}}{\partial q_i}\frac{\partial}{\partial q_j}\right)+\hat{V}, \tag{3}$$

where n again is the number of internal coordinates. It was solved variationally for the eigenvalues and eigenvectors with free-rotor and harmonic oscillator bases for the torsion and wagging coordinates.

TABLE II. Observed and calculated [MP2/6-31G(p,d)] torsional levels in the S_0 state. Kinetic and potential expansion coefficients (cm^{-1}).

v	Calc.		Obs.
0	0.0		
1	683.65		640.722[a]
2	1337.96		1307[b]
3	1871.84		
4	1960.81[c]	0.00[e]	
5	2549.72[c]	588.91[c]	503[c,d]
Terms	V^0	B^0	
constant	3010.82	24.0385	
$\cos(\theta)$	−848.17	1.1122	
$\cos(2\theta)$	−2018.75	−0.0777	
$\cos(3\theta)$	−132.47	−0.1812	
$\cos(4\theta)$	−4.55	−0.0353	

[a]anti from Ref. 13.
[b]anti from Ref. 14.
[c]syn conformer.
[d]From Ref. 15.
[e]1960.81 cm^{-1} set to 0.0 energy for syn.

IV. RESULTS AND DISCUSSIONS

A. The S_0 electronic state

In the S_0 ground state, a partial double bonding across the central O–C bond has the effect of impeding the free internal rotation of the OH group. Formic acid thus is stabilized into two planar rotamers (conformers), anti and syn by an energy barrier that prevents their interconversion. As the CHO formyl end of the molecule is rigidly planar in the lower electronic state, it is possible to treat the torsional motion independently from the remaining vibrational modes. We began with a one dimensional analysis of the potential energy associated with the internal rotation of the OH group by the *ab initio* HF method at different levels of approximation. Total energies were calculated for values of the torsional angle θ ranging between 0–360°, while the wagging coordinate was fixed at its planar value, $\alpha=0$. All of the other structural coordinates were fully relaxed. These optimized energy data points were fitted to terms in a Fourier expansion up to $\cos(4\theta)$ to form the potential energy $V(\theta)$. Expansion coefficients are given in the lower part of Table II.

Figure 4 shows the calculated potential function. A G2 calculation[10] predicts that the antirotamer of HCOOH is stabilized by 1465 cm^{-1} over the syn form. This value is in excellent agreement with a high-level extrapolation treatment made by Schaefer and co-workers[16] who estimated an energy separation of 1440 cm^{-1} between the two forms. The most reliable experimental value comes from the temperature variation of the microwave line strengths by Hocking *et al.*[17] Their measurements of the microwave line intensities placed the energy difference between the two conformers at the somewhat lower value of 1365 cm^{-1}. For the forward anti-syn process our G2 calculations predict a barrier height of 4468 cm^{-1}.

The calculated energy levels along with the kinetic and potential energy expansion coefficients are given in Table II. The arrangement of the levels within the torsional potential is illustrated in Fig. 4. The first 683.65 cm^{-1} interval calcu-

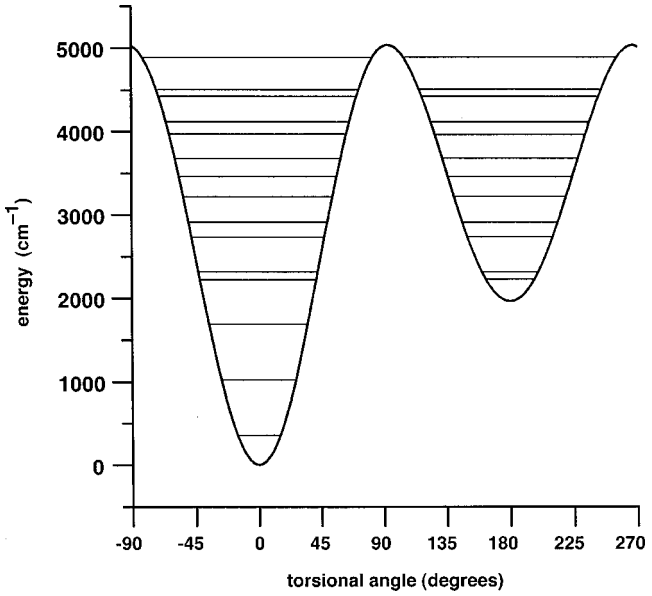

FIG. 4. The Q_9 torsional potential for the S_0 state. MP2/6-31G(d,p) basis, all coordinates relaxed. The wagging coordinate was fixed at its planar value, $\alpha=0°$, while all other coordinates were optimized other than the torsional angle, θ.

TABLE III. Observed (S_1) and calculated[a] torsional levels, kinetic, and potential expansion coefficients (cm^{-1}).

v	Calc.	Obs.
0	0.00	0.00
1	209.54	250.8[b]
2	314.81	377.2[b]
3	455.47	513.6[c]
4	581.61	
5	665.35	
Terms	V^0 (potential coeff.)	B^0 (kinetic coeff.)
constant	579.40	23.02
cos(θ)	−68.25	1.0070
cos(2θ)	14.82	0.3137
cos(3θ)	124.03	
cos(4θ)	12.36	
cos(5θ)	5.77	
sin(θ)	−459.57	
sin(2θ)	36.17	
sin(3θ)	−23.99	
sin(4θ)	38.40	
sin(5θ)	6.73	

[a]For T_1.
[b]From Ref. 5.
[c]From Ref. 4.

lated for the antirotamer manifold can be correlated with the infrared ν_9 fundamental[13] at 640.722 cm^{-1}. The second quantum of torsion, $2\nu_9$, has been observed in the gas phase Raman spectrum[14] at 1307 cm^{-1} and is +26 cm^{-1} above the expected position for a harmonic vibration. The present calculations show that the anharmonicity between the first and second quanta should be about −24 cm^{-1}. The calculations thus support the earlier suggestion[14] that the $v=2$ level of the Q_9 mode is severely perturbed by Fermi resonance.

The calculated level separations in the syn manifold are smaller than in those of the antirotamer. By inducing an anti→syn conversion through optically pumping the ν_1(OH) antifundamental, Pettersson *et al.* were able to observe an infrared spectrum of this unstable conformer.[15] Their reported 503 cm^{-1} value for the ν_9 syn-torsional fundamental is lower than the calculated 588.9 cm^{-1} value of Table II.

B. The S_1 excited electronic state

As a starting point for the analysis of the S_1 level structure, UMP2/6-31G(d,p) *ab initio* calculations were carried out on the companion T_1 triplet $n\pi^*$ state. Only several thousand cm^{-1} separate the S_1 and T_1 singlet and triplet states and it would be expected that the structures and torsion-wagging dynamics in the two states would be similar. This similarity allowed the energy levels calculated for the T_1 state to be used as the starting point for a comparison to the S_1 experimental data and the refinement of the spectroscopic constants. Calculations were performed on the T_1 state rather than the S_1 state because of limitations in the *ab initio* methodology and in the GAUSSIAN software. Analytical derivatives are not available for optimizing the structures of excited singlet states and the numerical evaluation is exceedingly slow. In our case it required over 150 optimized structures to define the potential function for the S_1 excited electronic state. We begin with a one-dimensional calculation of the torsional motion with the wagging angle fully relaxed. Terms up to cos(5θ) and sin(5θ) were included in the expansion to account for the shift in the position of the minimum position and the undulating nature of the potential. Table III gives the energy levels and expansion coefficients. From the potential function of Fig. 5 it is apparent that the barrier to OH torsion at 680 cm^{-1} is much lower in than the ground state 1440 cm^{-1} value.[16] But more importantly, the function contains only one minimum of any depth with an equilibrium coordinate shifted by $\theta=63.89°$. Thus, the somewhat surprising result that the minimum in the ground state becomes a maximum in the excited state. From the stack of energy

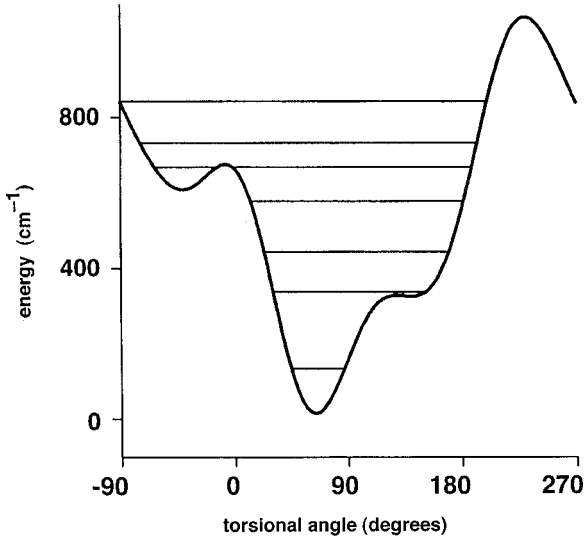

FIG. 5. The potential function for the Q_9 torsional coordinate in the upper excited electronic state.

TABLE IV. Potential[a] and kinetic[b] energy expansion coefficients for the S_1 excited electronic state (in cm^{-1}).

Coeff.[c] V	$B_{\theta,\theta}$	$B_{\theta,\alpha}$		
constant	−0.318 813+04	0.219 00+02	0.415 27+01	0.237 99+02
α^2	0.646 123 4+00	−0.891 00−04	−0.286 00−03	−0.439 00−04
α^4	0.619 763 9−04	0.563 00−07	0.151 00−07	
$\cos(\theta)$	−0.144 924 2+02	−0.174 50−02	0.162 90+01	0.156 09+01
$\cos(2\theta)$	−0.125 324 8+03	0.202 87+00	0.122 51+00	0.414 49+00
$\cos(3\theta)$	0.230 176 4+03			
$\alpha \sin(\theta)$	−0.243 314 9+00		−0.528 62−02	
$\alpha \sin(2\theta)$	0.974 639 1+01			
$\exp(-c\alpha^2)$	0.802 439 0+04			
$\exp(-c\alpha^2)\cos(\theta)$	−0.111 115 6+03			
$\exp(-c\alpha^2)\cos(2\theta)$	−0.606 229 5+03			
$\exp(-c\alpha^2)\cos(3\theta)$	−0.878 690 2+02			
$\alpha^3 \sin(\theta)$	−0.525 603 7−02			
$\alpha^3 \cos(2\theta)$	−0.303 885 2−02			
$\alpha^2 \cos(\theta)$			−0.508 00−04	

[a]From the morphed potential surfaces.
[b]From the MP2/6-31G(d,p) optimized structures.
[c]c was fixed at 6.50×10^{-4}.

levels, it is apparent that the zero point level rests in a V-shaped region of the potential, whereas for the second and third levels the function opens to three times its width. The remarkable anharmonicity is not too surprising as the fundamental at 250.8 cm^{-1} is observed to drop to nearly one half its value, 126.4 cm^{-1} to form the overtone.

V. TWO-DIMENSIONAL TREATMENT

The one-dimensional plot of Figs. 4 and 5 treat the symmetry of the S_0 ground state by the representations of C_s point group and the S_1 excited state by those of the C_1 group. These differing symmetries can be brought into alignment by using the G_2 nonrigid symmetry group for each electronic state. This requires that both the torsion and wagging vibrations be treated collectively by a two-dimensional model with the θ and α angles of Fig. 3 taken as variables. In the θ direction the potential for the upper electronic state was described by the Fourier series $\cos(\theta)$, $\cos(2\theta)$, and $\cos(3\theta)$ over the full 360° rotation. The double minimum in the potential function in the α direction required the use of the Coon function.[18] This is constructed from a Gaussian term, $\exp(-c\alpha^2)$, that describes the central barrier while the outer edges of the two wells are formed from the addition of quadratic-quartic terms, α^2 and α^4. The two internal coordinates were coupled by the cross terms $\alpha \sin(\theta)$, $\alpha \sin(2\theta)$, $\alpha^2 \cos(\theta)$, $\alpha^3 \sin(\theta)$, $\alpha^3 \cos(2\theta)$, $\exp(-cx^2)\cos(\theta)$, $\exp(-cx^2)\cos(2\theta)$, and $\exp(-cx^2)\cos(3\theta)$. In all, 15 expansion terms provided an adequate fit to the *ab initio* energy data points. The excited state potential and kinetic expansion coefficients are given in Table IV.

Nonrigid group theory[19] was used for the labeling the energy levels, factorization of the Hamiltonian matrix and the generation of the selection rules. The existence of the O–C═O plane of symmetry allows the S_0 and S_1 structures to classified according to the $\hat{S}$ switch operation,

$$\hat{S}f(\theta,\alpha)=f(-\theta,-\alpha) \tag{4}$$

and creates a nonrigid G_2 group that is isomorphous to the C_S point group. This summarization allows the torsion-wagging functions to be classified according to the symmetry species: a' (in-plane) and a'' (out-of-plane).

The calculated energy levels were adjusted to fit the observed levels by morphing the potential energy surface that was initially obtained from the *ab initio* procedure. The refinement was carried out by minimizing the differences between the calculated and observed levels by a quasi-Newton method.[20] Throughout the fitting process, the kinetic energy expansion coefficients were fixed at their *ab initio* values. The morphing operation, where the calculated and observed levels are forced into agreement, was adopted from the same procedure whereby molecular structures (bond lengths and angles) are optimized through the lowering of the total electronic energy. Thus, for the case of *ab initio* optimizations there are many parameters, bond lengths, and angles that must be determined from a single observable, the total energy. In our case, it is the expansion coefficients in the potential function that are determined by minimizing the sum of the squares of the residuals between the observed and calculated levels. This is not a least squares procedure as there are many more parameters (expansion coefficients) than observable (levels). Consequently, for this process to be successful, the initial analytical potential derived from the *ab initio* HF calculations must be sufficiently close to the true potential that the system does not morph into a false minimum.

Table V gives the energy levels calculated from the UMP2/6-31G(d,p) procedure. The modest agreement between these levels and the observed levels should not come as a great surprise as the *ab initio* calculations are for the companion $T_1(n\pi^*)$ state. On morphing the potential surface by adjusting the potential energy expansion coefficients, a nearly perfect fit is reached with the observed levels. The greatest mismatch is between the observed and calculated $v=1$ torsional levels (250.83 and 196.92 cm^{-1}, respectively) and accordingly the morphing adjustment is greatest in the θ

TABLE V. Relative band positions (displacements from T_0) for the a/b- and c-type transitions from the morphed S_1 potential energy surface.

vib. quanta		c-origin		a/b-origin			
tor.	wag	obs.[a]	UMP2	morph.	obs.[a]	UMP2	morph.
0	0	0.0	0.00	0.00	0.00	0.00	0.00
1	0	250.83	196.92	250.83	250.83	196.92	250.85
2	0	377.20	350.80	377.22	377.50	350.80	377.51
3	0	513.6[b]	488.07	513.99	513.6[b]	488.08	514.45
4	0		585.88	671.59		585.92	672.07
5	0		636.21	809.91		636.16	810.26
0	1	866.3	742.71	866.30	866.81	742.76	866.02
6	0		835.39	985.93		835.40	986.07

[a]In cm^{-1}.
[b]Interval measured from bandheads.

direction. The overall shape of the morphed potential surface for the S_1 excited state is similar to that calculated by the UMP2/6-31G(d,p) procedure. The *ab initio* calculations placed the global minimum for the stable anticonformer at $+71.2$ and $+47.6$ for the θ and α angles, which on morphing shifted to $+68.08°$ and $+57.51°$. For the unstable syn conformer, the θ and α angles shifted on morphing form $+52.0$ and -39.5 to $+48.50°$ and $-44.77°$, respectively.

As stated earlier, symmetry considerations require that nonrigid formic acid be classified as G_2, which is isomorphous to the C_s point group. Given that the first excited state has electronic symmetry a'' symmetry, then the transitions labeled as c-type have upper state symmetry a'' while those labeled as a/b-type have symmetry a'. Molecules with a single inversion motion, analogous to the υ_8 vibration in formic acid, would alternate band types starting with a c-type band followed closely by an a/b-type band with the a/b-type band always higher in frequency. Inspection of Table V for the one quantum of the υ_8 vibration shows an apparent anomaly, in that the calculated, morphed a/b-type band is lower in frequency than the c-type band, i.e., an inverted pair. In reality, this apparent inversion is to be expected based on symmetry arguments and the computer simulation gives the correct ordering.

The molecule has two large amplitude inversion motions and both are required to invert the molecule (as required by the switch operation, S). However, the normal modes are labeled as wag and torsion, and there is uncertainly as to which mode actually shows or carries the inversion splitting that one ascribes the traditional $(+/-)$ label. We performed a study of this feature by producing a correlation diagram that is depicted in Fig. 6. Here the right-hand side shows the splittings for two identical double minimum functions while the left-hand side shows the pattern for a double minimum function and a single minimum function. We have chosen to label the changing function as a wag (W). One starts with a set of parameters that give a reasonable splitting to the levels of the two double minimum functions. Symmetry arguments confirm the computer calculation that the lower set of four levels is composed of two singly degenerate levels of different symmetry and a middle double degenerate level. The next higher grouping is predicted to be composed of four levels with two singly degenerate levels of the same symmetry and a higher frequency doubly degenerate level. When the symmetry is relaxed and one of the double minimum functions is allowed to move to a pure quartic oscillator (single minimum), the lowest 0^+ and 0^- pair of inversion levels remains unchanged (with separation Δ_0) while the other pair climbs to its quartic oscillator frequency while maintaining the Δ_0 splitting of the lower pair. A smooth correlation is required throughout the process. Thus, the predicted pattern for the four lowest levels has the inversion

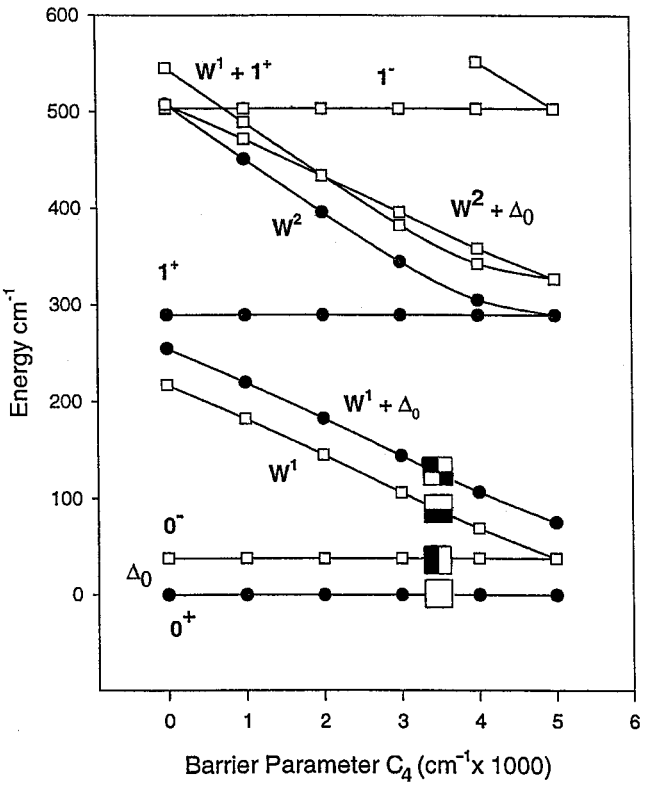

FIG. 6. An energy diagram of the vibrational levels correlated between a double minimum-single minimum (DM-SM), $V(x,y)-C_1x^4-C_2x^2+C_3y^4$ and a double minimum-double minimum (DM-DM), $V(x,y)=C_1x^4-C_2x^2+C_3y^4-C_4y^2$ as a function of the C_4 barrier parameter. For these model systems $C_1=C_3=20\,000\ cm^{-1}$ and $C_2=5000\ cm^{-1}$. The kinetic terms were set equal to each other, $B_{11}=B_{22}=5.0\ cm^{-1}$ and decoupled, $B_{12}=0.0\ cm^{-1}$. The nodal properties of the four lowest energy wave functions are shown as checkerboard rectangles.

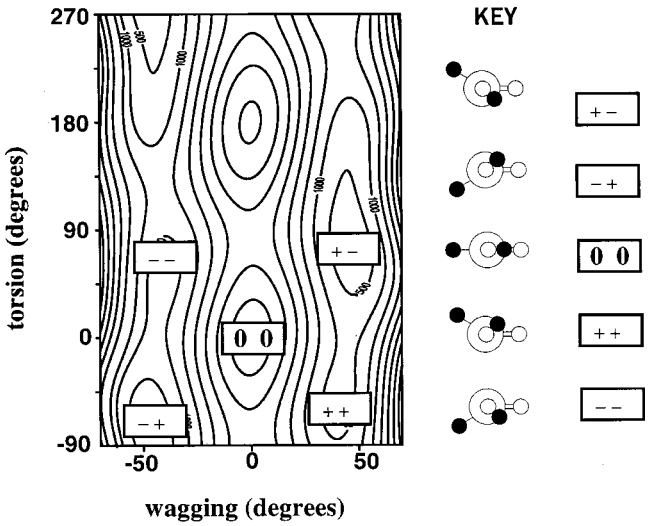

FIG. 7. The S_1 excited state potential energy surface, $V(\theta,\alpha)$, contour intervals at 500 cm^{-1}. Newman projection diagrams for the regions morphed from the observed vibrational data.

splitting for the lower pair as *c*-type followed by *a*/*b*-type while the upper pair is split with the *a*/*b*-type band of lower frequency. The pattern at higher energy is more difficult to follow since the levels become congested but here the pattern for double quantum addition of wag has the type *c* band lower in frequency than the *a*/*b*-type. Thus, in assigning the spectra of molecules that have two isomers each with a double minimum, the mode with the deeper well depth should be chosen as the inversion motion (for the purposes of assigning the +/− label) and the other normal mode as a simple single minimum oscillator. The symmetry assignments of the levels then follow exactly as if only one double minimum mode is present. Note that in our Fig. 2 of Ref. 5, we have incorrectly chosen ν_8 (wag) as the carrier of inversion, rather, based on the arguments presented above, it is ν_9 (torsion) that carries the inversion.

VI. DISCUSSION

A comparison of the $V(\theta,\alpha)$ potentials for the ground and excited electronic states immediately lead to an appreciation of the conformational changes that occur on excitation. A useful way to interpret the contours on an energy diagram is by the use of Newman projection diagrams. These are pictorial representations of formic acid viewed along the C–O single bond axis, where the C═O double bond projects from the axis in a horizontal direction. The torsion of the OH group is represented by a circle describing the rotation of the hyroxy hydrogen while the wagging position is illustrated by the acetyl hydrogen atom that swings in an arc above and below the O–C═O plane. The morphed excited state potential along with the Newman projections are illustrated in Fig. 7.

To label the regions of the contour diagram we use a + and − notation that describes the positions of the hydrogen atoms with respect to the O–C═O plane. Thus, in the stable equilibrium structure, the hydroxy hydrogen lies above the plane and the acetyl hydrogen below the plane and the torsion-wagging coordinates (θ,α) are designated $(+,-)$. A second stable conformer $(-,+)$ is connected through the switch operator that simultaneously changes the signs of both angles. These two inversion partners can be correlated with global minima in the potential surface. The contour lines in the center of the diagram are also closely spaced and they indicate the presence of a potential maximum that corresponds to the planar configuration (0,0) where the two angles assume zero values. The upper left and the lower right corners of the potential surface are also indicative of points of stability. These points correspond to the structures $(+,+)$ and $(-,-)$ where the O–H and C–H bonds project from the same side of the O–C═O frame. Thus the two-dimensional energy surface reveals that there are four conformers grouped into pairs that are related to each other by a switching (reversal) of their coordinates, $(+,-)\leftrightarrow(-,+)$ and $(+,+)\leftrightarrow(-,-)$. It is this inversion process that is responsible for the splitting of the levels into doublets. The height of the global barrier, in turn, is directly related to the inversion doubling separations.

The morphing procedure that brings the levels generated by the UMP2 calculations into agreement with the observed data place the $(+,-)$ conformer at a well depth of 5275 cm^{-1} relative to the top of the barrier (0,0) position with equilibrium positions $\theta=+68.08°$ and $\alpha=-57.51°$. A rotation of the OH group through the O–C═O plane creates a second region of stability $(+,+)$ at $\theta=-48.50°$ and $\alpha=+44.77°$. This second conformer lies 1207 cm^{-1} above the $(+,-)$ conformer and is separated by a saddle point at 1270 cm^{-1}.

The torsional wagging surface can only be studied by LIF spectroscopy in a region of $\pm 60°$ in the θ and α directions from the stable anti (0,0) conformation of the lower S_1 state. Thus, the upper part of the $V(\theta,\alpha)$ surface would require vibronic transition data from the syn (180,0) ground state conformer, and hence is not probed by the LIF technique. The shape of the potential in this region depends on the quality of the UMP2 calculations.

ACKNOWLEDGMENTS

The authors are very grateful to the National Research Council of Canada and the Office of Basic Energy Sciences of the U.S. Department of Energy for financial support. Acknowledgment is made to the donors of The Petroleum Research Fund, administered by the ACS, for partial support of this research.

[1] R. C. Millikan and K. S. Pitzer, J. Chem. Phys. **27**, 1305 (1957).
[2] B. Sugarman, Proc. Phys. Soc. London **55**, 429 (1943).
[3] T. L. Ng and S. Bell, J. Mol. Spectrosc. **50**, 166 (1974).
[4] F. Ioannoni, D. C. Moule, and D. J. Clouthier, J. Phys. Chem. **94**, 2290 (1990).
[5] L. M. Beaty-Travis, D. C. Moule, H. Liu, E. C. Lim, and R. H. Judge, J. Mol. Spectrosc. **205**, 232 (2001).
[6] L. M. Beaty, D. C. Moule, C. Muñoz-Caro, and A. Niño, *New Trends in Quantum Systems in Chemistry and Physics*, edited by J. Maruan (Klewer Academic), **1**, 347 (2001).
[7] G. Fischer, J. Mol. Spectrosc. **29**, 37 (1969).
[8] R. H. Judge and D. C. Moule, J. Mol. Spectrosc. **113**, 302 (1985).
[9] M. Brouard, J. P. Simon, and J.-X. Wang, Faraday Discuss. Chem. Soc. **91**, 63 (1991).

[10] M. J. Frisch, G. W. Trucks, H. B. Schegel *et al.*, GAUSSIAN 95, Gaussian, Inc., Pittsburgh, Pennsylvania, 1995.
[11] A. Niño and C. Muñoz-Caro, Comput. Chem. (Oxford) **56**, 27 (1994).
[12] H. M. Pickett, J. Chem. Phys. **56**, 1715 (1972).
[13] J-C. Deroche, J. Kauppinen, and E. Kyrö, J. Mol. Spectrosc. **78**, 379 (1979).
[14] J. E. Bertie and K. H. Michaelian, J. Chem. Phys. **76**, 886 (1982).
[15] M. Petteresson, J. Lundell, L. Khriachtchev, and M. Räsänen, J. Am. Chem. Soc. **119**, 11715 (1997).
[16] A. G. Császár, W. D. Allen, and H. F. Schaefer III, J. Chem. Phys. **108**, 9751 (1998).
[17] W. H. Hocking, Z. Naturforsch. A **31a**, 1113 (1976); E. Bjarnov and W. H. Hocking, *ibid.* **33a**, 610 (1978).
[18] J. B. Coon, N. W. Naugle, and R. D. McKenzie, J. Mol. Spectrosc. **20**, 107 (1966).
[19] Y. G. Smeyers, Adv. Quantum Chem. **24**, 1 (1992).
[20] R. Fletcher, *Practical Methods of Optimization* (Wiley, New York, 1987), Chap. 3.